

Supporting Information

In Situ NMR Study on the Interaction between LiBH_4 – $\text{Ca}(\text{BH}_4)_2$ and Mesoporous Scaffolds

Hyun-Sook Lee,[†] Son-Jong Hwang,^{‡} Hoon Kee Kim,[‡] Young-Su Lee,^{*†} Jinsol Park,[§] Jong-
Sung Yu,[§] and Young Whan Cho[†]*

[†]High Temperature Energy Materials Research Center, Korea Institute of Science and
Technology, Seoul 136-791, Republic of Korea

[‡]Division of Chemistry and Chemical Engineering, California Institute of Technology,
Pasadena, California 91125, United States

[§]Department of Advanced Materials Chemistry, WCU Research Center, Korea University,
208 Seochang, Jochiwon, Chungnam 339-700, Republic of Korea

*Corresponding authors: Son-Jong Hwang E-mail: sonjong@cheme.caltech.edu Tel: +1-626-
395-2323; Young-Su Lee E-mail: lee0su@kist.re.kr Tel: +82-2-958-5412.

Supporting Information: Figure 1 and Figure S1 present ^{11}B , ^1H , and ^7Li MAS NMR spectra for the ball-milled LC (black) and LC/CMK-3 (red). In all ^{11}B NMR spectra of LC and LC/CMK-3, there appear minor and broad peaks at ~ 0 ppm and ~ 5 -20 ppm, which are related to B-O bondings in $\text{B}(\text{OH})_4$ and BO_3 groups, respectively.¹⁻² We observed the same peaks mainly in the starting material of $\text{Ca}(\text{BH}_4)_2$, indicating the presence of the oxide contaminants in the as-received chemicals to some extent. The oxygen contamination of $\text{Ca}(\text{BH}_4)_2$ is responsible for the formation of unexpected intermediate phases³⁻⁴ like $\text{Ca}_3(\text{BH}_4)_3(\text{BO}_3)$ and $\text{LiCa}_3(\text{BH}_4)(\text{BO}_3)_2$. However, the amount is less than 5 % of the total LC or LC/CMK-3 materials, which would not change the main results in our study. The line broadening observed for all nuclei in LC/CMK-3 compared to LC can be explained with the distorted local magnetic field homogeneity because of anisotropic magnetic susceptibility of CMK-3 and/or higher disorder in materials due to dispersion of borohydrides over large surface area.⁵ The shifted peaks, upfield in particular and clear at least for ^1H and ^7Li NMR, could be originated from interaction of borohydrides with carbon surface⁶ that is mainly composed of aromatic rings. The local circulation of electrons around aromatic rings can shield the external magnetic field experienced at nucleus and leads shift to upfield.⁷ Those NMR results certainly indicate that only part of borohydrides is in close contact with carbon surface after ball-milling.

Experimental Section:

The eutectic $0.68\text{LiBH}_4+0.32\text{Ca}(\text{BH}_4)_2$ composites (LC) were made by mixing as-purchased commercial LiBH_4 (assay 95%, Acros) and $\text{Ca}(\text{BH}_4)_2$ (assay 98%, Sigma-Aldrich). Various scaffolds were used to create different kinds of interface: mesoporous carbon (CMK-3), mesoporous silica (MCM-41, Sigma-Aldrich), microporous pure silica zeolite, and non-porous graphite and quartz glass powder. CMK-3 (pore size of 3.5 nm, BET surface area of

1229 m²/g, and mesopore volume of 1.04 cm³/g) was synthesized using a mesoporous silica SBA-15 as a template and phenol as a carbon source.³ To remove residual oxygen or water, the CMK-3 was dried at 420 °C under vacuum for 6 h before using. Commercial MCM-41 (Sigma-Aldrich, pore size of 2.1-2.7 nm, pore volume of 0.98 cm³/g, used after dried at 200 °C under vacuum for 5 h to remove water) and graphite powder (99.99%, Sigma-Aldrich) were used. Microporous pure silica zeolite beta was prepared and calcined in the Professor Davis group at California Institute of Technology using well established recipe.⁸ The calcined zeolite beta showed the micropore volume of 0.19 cm³/g and was used after the similar pretreatment to remove water. Hereafter, we will use a notation such as LC/CMK-3 for denoting the eutectic LC mixture with CMK-3. For the LC/CMK-3 sample, the amount of carbon was chosen such that its mesopore volume is equal to the calculated volume of the bulk LC composite. The amount of other scaffold materials used was adjusted similarly. The samples were prepared by ball-milling or hand-mixing (mortar and pestle), and in some cases subsequent melt-infiltration was done. A ball-milling process was conducted using a planetary mill (Fritsch P7) operated at 600 rpm for 1 h. About 1 g of the mixture was ball-milled together with three 12.7 mm and seven 7.9 mm diameter Cr-steel balls. For melt-infiltration, the mixtures were heated at 230 °C for 30 min under $p(\text{H}_2) = 3$ bar and cooled down to room temperature. The temperature of 230 °C was chosen to be over the eutectic melting point of LC (~200 °C)³ to ensure full melt-infiltration. Sample handling was done in an argon-filled glove box whenever needed (LABstar, MBraun, $p(\text{O}_2) < 1$ ppm).

Multinuclear magic angle spinning nuclear magnetic resonance (MAS NMR) measurements were performed using a Bruker DSX-500 spectrometer and a Bruker 4 mm wide variable temperature (WVT) MAS probe which is free of boron background. The operating frequencies for ¹H, ¹¹B, ⁷Li are 500.2, 160.5, and 194.4 MHz, respectively. Samples were

loaded into 4 mm ZrO₂ rotors and sealed with Vespel drive caps inside an argon-filled glove box. Quartz glass powder was often ground with a sample as a diluting agent using a mortar and a pestle when the electrically conducting nature of samples caused severe probe detuning problems. Compressed dry N₂ gas was used for sample spinning, and the speeds were typically 15 kHz for *ex situ* and 8 kHz for *in situ* variable temperature (VT) experiments. NMR signals were acquired after single pulse, 4 μs-90 degree pulse for ¹H and 0.5 μs-π/12 for ¹¹B or ⁷Li, and strong ¹H decoupling pulse was used for ¹¹B and ⁷Li detections. NMR spectra were referenced to external references of tetramethylsilane (TMS), BF₃·O(CH₂CH₃)₂, 1M aqueous solution of LiCl, for ¹H, ¹¹B, and ⁷Li, respectively. In addition, the NMR experiments for LC/MCM-41 were performed in two different ways because of repeated spinning crashes (cap opening due to high pressure building inside) during *in situ* NMR (Fig. 3(a)) at temperature above 140 °C. NMR recording for higher temperatures was performed in *ex situ* (Fig. 3(b)). For this case, a hand mixed LC/MCM-41 was heated under 1 bar of Ar gas for 2 hours and cooled for NMR measurements.

Thermogravimetric analysis (TG, Netzsch TG 209 F1) combined with mass spectrometry (MS, Netzsch QMS 403 C) was done for LC mixed with carbon materials. The TG-MS data were obtained while heating a sample to 500 °C at a scanning rate of 5 °C/min under flowing argon (99.9999% purity, 40 mL/min).

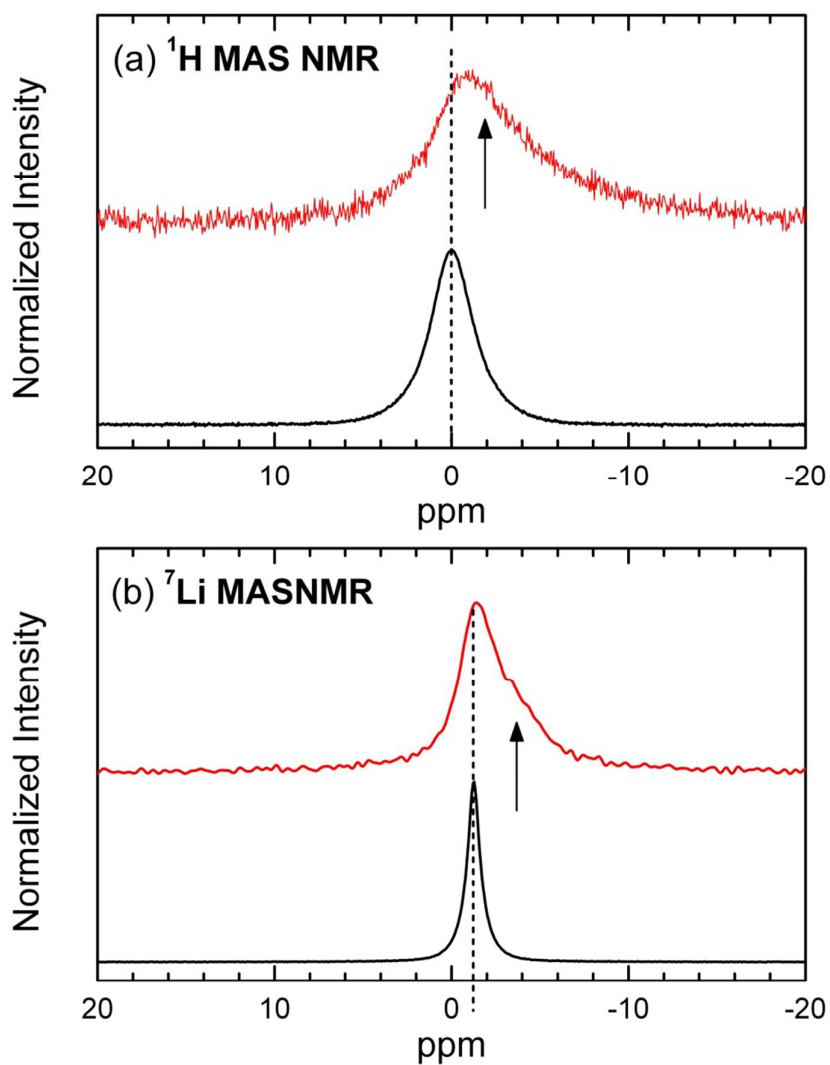


Figure S1. *Ex situ* (a) ^1H , and (b) ^7Li MAS NMR spectra of the ball-milled $0.68\text{LiBH}_4+0.32\text{Ca}(\text{BH}_4)_2$ without CMK-3 (black) and with CMK-3 (red). The new peaks are marked by the arrows.

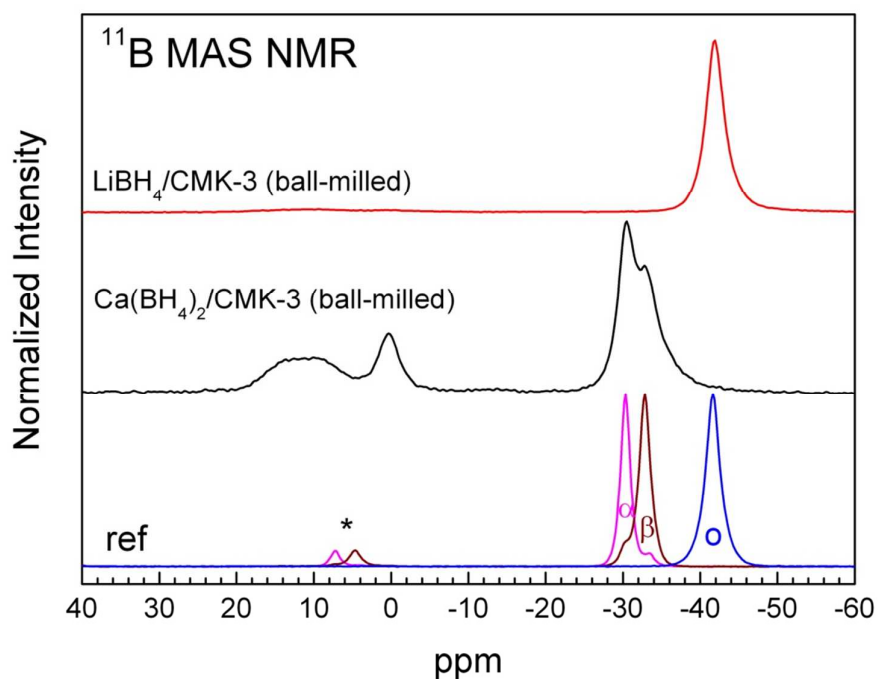


Figure S2. *Ex situ* ^{11}B MAS NMR for the ball-milled samples of $\text{LiBH}_4/\text{CMK-3}$ and $\text{Ca}(\text{BH}_4)_2/\text{CMK-3}$. The symbols “ α ”, “ β ”, and “ \circ ” denote $\alpha\text{-Ca}(\text{BH}_4)_2$, $\beta\text{-Ca}(\text{BH}_4)_2$, and orthorhombic LiBH_4 , respectively. No new peak is observed in these two samples. The peaks located at 0-20 ppm originated from the oxygen-containing groups of $\text{B}(\text{OH})_4$ and BO_3 are observed only in $\text{Ca}(\text{BH}_4)_2$. Spinning sidebands are marked by the *.

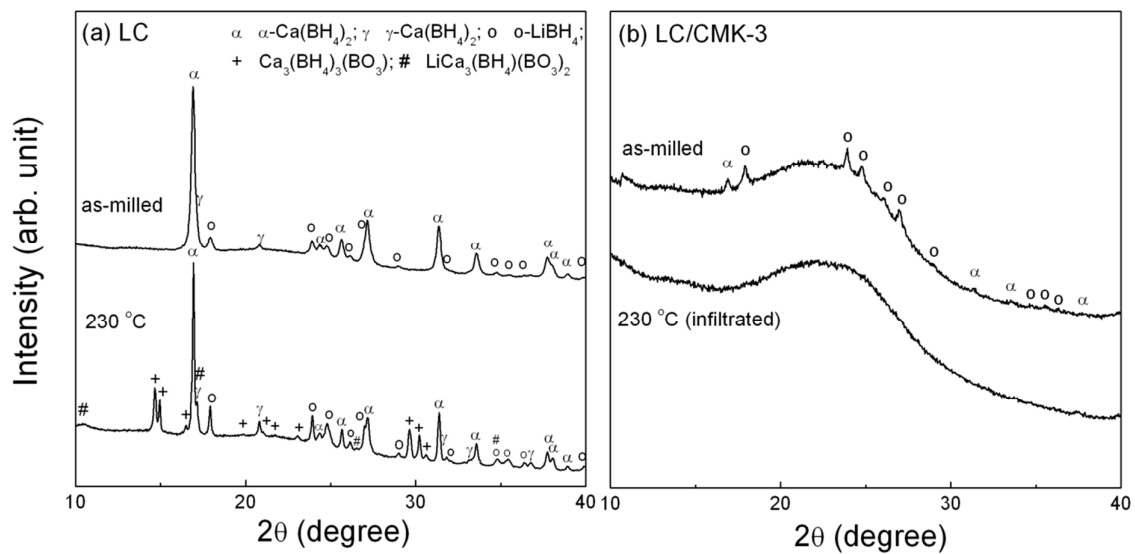


Figure S3. XRD patterns of the ball-milled 0.68LiBH₄+0.32Ca(BH₄)₂ without carbon (a) and with carbon (b). The infiltrated samples were treated at 230 °C for 30 min under 3 bar of hydrogen pressure.

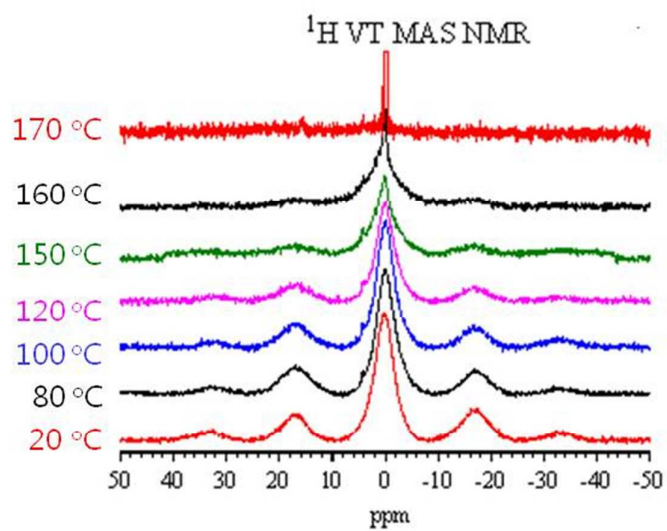


Figure S4. *In situ* ^1H MAS NMR spectra of the eutectic mixture of $0.68\text{LiBH}_4+0.32\text{Ca}(\text{BH}_4)_2$ in the absence of CMK-3.

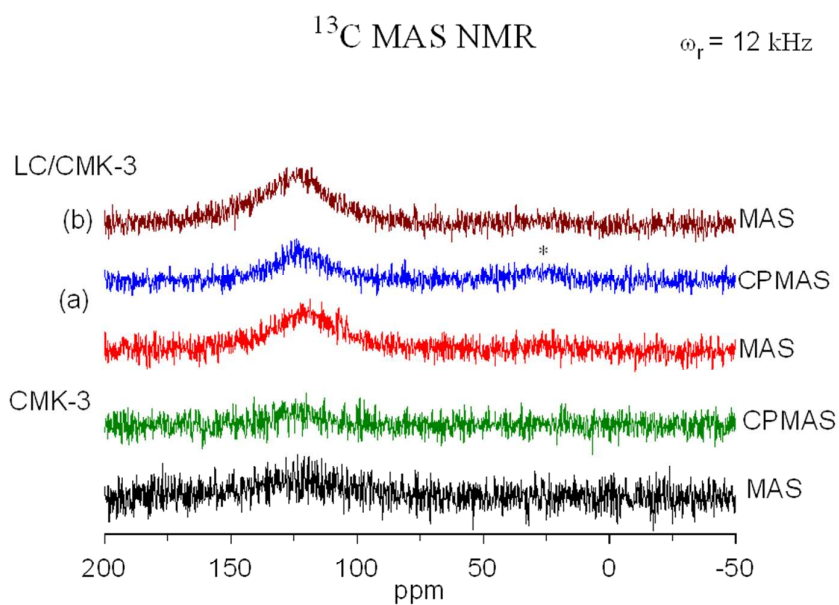


Figure S5. *Ex situ* ^{13}C Bloch Decay MAS and CPMAS NMR spectra of CMK-3 only and of the eutectic mixture $0.68\text{LiBH}_4+0.32\text{Ca}(\text{BH}_4)_2$ with CMK-3: infiltrated at $230\text{ }^\circ\text{C}$ (a) and dehydrogenated at $400\text{ }^\circ\text{C}$ (b). Peak near 125 ppm indicates that nearly all carbons are in graphite like environment (C=C double bonds). No aliphatic peak appears after infiltration or dehydrogenation reactions, showing the non-reactive nature of the carbon surface with borohydrides unlike fullerenes. Spinning sidebands are marked by the *.

References:

- (1) Soraru, G. D.; Dallabona, N.; Gervais, C.; Babonneau, F., Organically Modified SiO₂-B₂O₃ Gels Displaying a High Content of Borosiloxane (= B-O-Si) Bonds. *Chem. Mater.* **1999**, *11*, 910-919.
- (2) Vanwullen, L.; Mullerwarmuth, W., B-11 Mas NMR-Spectroscopy for Characterizing the Structure of Glasses. *Solid State Nucl. Mag.* **1993**, *2*, 279-284.
- (3) Lee, H.-S.; Lee, Y.-S.; Suh, J.-Y.; Kim, M.; Yu, J.-S.; Cho, Y. W., Enhanced Desorption and Absorption Properties of Eutectic LiBH₄-Ca(BH₄)₂ Infiltrated into Mesoporous Carbon. *J. Phys. Chem. C* **2011**, *115*, 20027-20035.
- (4) Lee, Y.-S.; Filinchuk, Y.; Lee, H.-S.; Suh, J.-Y.; Kim, J. W.; Yu, J.-S.; Cho, Y. W., On the Formation and the Structure of the First Bimetallic Borohydride Borate, LiCa₃(BH₄)(BO₃)₂. *J. Phys. Chem. C* **2011**, *115*, 10298-10304.
- (5) Verkuijlen, M. H. W.; Gao, J.; Adelhelm, P.; van Bentum, P. J. M.; de Jongh, P. E.; Kentgens, A. P. M., Solid-State NMR Studies of the Local Structure of NaAlH₄/C Nanocomposites at Different Stages of Hydrogen Desorption and Rehydrogenation. *J. Phys. Chem. C* **2010**, *114*, 4683-4692.
- (6) Huwe, H.; Froba, M., Iron(III) Oxide Nanoparticles within the Pore System of Mesoporous Carbon CMK-1: Intra-Pore Synthesis and Characterization. *Micropor. Mesopor. Mater.* **2003**, *60*, 151-158.
- (7) Anderson, R. J.; McNicholas, T. P.; Kleinhammes, A.; Wang, A.; Liu, J.; Wu, Y., NMR Methods for Characterizing the Pore Structures and Hydrogen Storage Properties of Microporous Carbons. *J. Am. Chem. Soc.* **2010**, *132*, 8618-8626.
- (8) Cambor, M. A.; Corma, A.; Valencia, S., Spontaneous Nucleation and Growth of Pure Silica Zeolite-Beta Free of Connectivity Defects. *Chem. Commun.* **1996**, 2365-2366.